Available online at www.sciencedirect.com
ScienceDirect
Journal of Sound and Vibration 307 (2007) 818–833
JOURNAL OF SOUND AND VIBRATION
www.elsevier.com/locate/jsvi

Semi-passive random vibration control based on statistics

D. Guyomar, C. Richard, S. Mohammadi*

Laboratoire de Génie Electrique et Ferroélectricité, INSA, Lyon, Bat. G. Ferrié, 69621 Villeurbanne Cedex, France

Received 18 December 2006; received in revised form 9 July 2007; accepted 12 July 2007
Available online 27 August 2007

Abstract

This paper considers the development of an enhanced control strategy for a semi-passive piezoelectric damping device (SSD or pulse switching). Following the proposed approach, the voltage or displacement signal is analysed during a given time window and the statistically probable displacement or voltage-level threshold is determined from both the average and standard deviation of the signal during the observation period. The voltage step still occurs on a local maximum of the signal but only above the statistically defined threshold. A significant decrease in vibration energy is demonstrated experimentally and theoretically in the case of a clamped beam excited by random noise. It is shown that in the case of multimodal vibration, all of the modes are controlled and preferentially those corresponding to the highest displacement amplitudes.

1. Introduction

Several methods have been investigated for semi-passive nonlinear vibration damping and energy reclamation using piezoelectric elements [1–3]. These methods are interesting because they do not rely on any operating energy as in active control. They consist of drive by a few solid-state switches (i.e. MOSFET transistor) requiring very little power. The common strategy of these methods consists of modification of the electric boundary conditions of the piezoelectric elements (open or short circuit). In the solid-state-tuneable piezoelectric absorber developed by Davis and Lesieutre [4], a passive capacitive shunt circuit is used to electrically adjust the effective stiffness of the piezoelements and then to tune the device resonance frequency out of the excitation bandwidth. The state switching method proposed by Clark [5] is a variable stiffness technique, in which piezoelements are periodically held in short circuit. Synchronised switch damping (SSD) techniques [6–8] which are implemented in this paper consist of leaving the piezoelements in open circuit except during a very brief period of time where the electric charge is either suppressed (SSDS) in a short circuit or inverted (SSDI) with a resonant network. The damping or energy reclamation performances depend strongly on the piezoelectric coupling coefficient and consequently this coefficient has to be maximised [9,10]. It was shown [11] that for a harmonic regime, optimal switching should occur on each extremum of the voltage or of the piezoelement strain. Corr and Clark [12] experimented with SSDI or pulse switching in the case of a

*Corresponding author. Tel.: +33 472 43 81 58; fax: +33 472 43 88 74.
E-mail address: saberm7@yahoo.com (S. Mohammadi).

0022-460X/$ - see front matter © 2007 Elsevier Ltd. All rights reserved.
doi:10.1016/j.jsv.2007.07.008

multimodal vibration. The proposed technique consists of selecting the modes to be controlled using numerical filtering techniques. Also, they showed that the original SSD control law was not optimal in the case of large band excitation.

In the case of large bands of excitation, the optimisation of piezoelectric elements (size and location) as well as the switching network is not sufficient. Using a nonlinear technique such as SSD is very important to operate the voltage-switching device exclusively on certain selected extrema [6,7]. As specified in the following, in the case of the SSD technique, the energy extracted from the structure by the piezoelement is proportional to Σv_k^2, where v_k is the piezoelectric voltage just before the kth switching sequence (short circuit or inversion). This paper proposes statistical analysis to define optimisation instants for the switching sequence in order to maximise the extracted energy and vibration damping. The proposed methods are based on a statistical evaluation of the voltage generated by the piezoelectric elements or of the structure deflection. In order to theoretically analyse the various statistical methods, a multimodal structure equipped with piezoelements wired on a SSDI switching cell was simulated and experimented.

Section 2 describes the multimodal model used for the simulation as well as the methods used for parameter identification in the experimental set-up. The energy balance equation of the system is also established. Section 3 lists and discusses the various control techniques. Control Probability Law (CPL) is detailed as well as the proposed statistical methods. Section 4 summarises the simulation results and gives a comparison of the various methods. Finally, it depicts the experimental set-up and results.

2. Theoretical model of the semi-passive piezoelectric device

2.1. Multimodal structure modelling

The differential equation for a beam with lateral motion is given by Eq. (1) [13] where $u(x,t)$ is the lateral beam deflection according to Fig. 1. E and J represent Young's modulus and the inertia moment of the cross-section, and ρ, c and $f(x,t)$ are the mass, damping and excitation force per unit length, respectively. This equation corresponds to Euler–Bernoulli assumptions.

$$\rho\frac{\partial^2 u(x,t)}{\partial t^2}+c\frac{\partial u(x,t)}{\partial t}+\frac{\partial^2}{\partial x^2}\left[EJ\frac{\partial^2 u(x,t)}{\partial x^2}\right]=f(x,t). \tag{1}$$

It is interesting to find the particular solution of Eq. (1) for a general excitation force per unit length. First, we assume that the excitation force is given by

$$f(x,t)=p(x)f(t), \tag{2}$$

where $p(x)$ is the load's spatial distribution and $f(t)$ is the input time history. Second, we assume that the particular solution is given by

$$u(x,t)=\sum_{i=1}^{N}\varphi_i(x)q_i(t), \tag{3}$$

where $q_i(t)$ and $\varphi_i(x)$ are the modal coordinates and the eigenmode functions, respectively. N is the number of modes. The eigenmode functions are also orthogonal thus satisfying the relations

$$\int_0^l \rho\varphi_i(x)\varphi_k(x)\,\mathrm{d}x=\begin{cases}0 & \text{for} \quad i\neq k,\\ M_i & \text{for} \quad i=k,\end{cases} \tag{4}$$

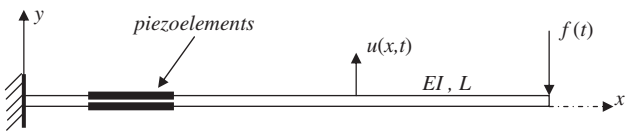

Fig. 1. Schematic diagram of cantilever beam. $u(x,t)$ is the beam deflection along the transverse direction (y) and $f(t)$ is the excitation force at the tip of the beam ($x=L$).

$$\int_0^l \frac{\mathrm{d}^2}{\mathrm{d}x^2}\left[EJ\frac{\mathrm{d}^2\varphi_i(x)}{\mathrm{d}x^2}\right]\varphi_k(x)\,\mathrm{d}x = \begin{cases} 0 & \text{for} \quad i \neq k, \\ K_i & \text{for} \quad i = k, \end{cases} \tag{5}$$

where M_i and K_i are the generalised mass and generalised stiffness for the ith mode, respectively, and l is the cantilever beam length. After insertion of Eqs. (2) and (3) into Eq. (1) and multiplying it by $\varphi_k(x)\,\mathrm{d}x$, integrating on length l and employing the orthogonality condition of Eqs. (4) and (5), along with assuming that damping is proportional to the mass and stiffness distributions, the result is

$$M_i\ddot{q}_i + c_i\dot{q}_i + K_i q_i = \bar{Q}_i f(t), \tag{6}$$

where $q_i(t)$ can be determined from these equations. c_i is the ith generalised damping coefficient and $\bar{Q}_i$ is the generalised excitation force [13] given by

$$\bar{Q}_i = \int_0^l p(x)\varphi_i(x)\,\mathrm{d}x. \tag{7}$$

For the cantilever beam problem represented in Fig. 1, the concentrated external force $f(t)$ is applied at the free-end of the beam and the piezoelectric patches are bonded on the structure. Eq. (6) becomes

$$M_i\ddot{q}_i + c_i\dot{q}_i + K_{ei}q_i = \varphi_i(l)f(t) - \alpha_i v_i(t), \tag{8}$$

where K_{ei} is the short-circuit generalised stiffness. The term $\alpha_i v_i(t)$ corresponds to the force due to ith component of the voltage according to the macroscopic piezoelectric coefficient α_i. These coefficients depend on the modes considered as well as the corresponding stress distributions. In the open-circuit condition, the piezoelectric voltage v_i due to the ith mode of vibration is

$$v_i = \frac{\alpha_i}{C_0}q_i(t). \tag{9}$$

The global piezoelectric voltage resulting from the mode superposition is

$$v = \frac{1}{C_0}\sum_{i=1}^{N}\alpha_i q_i(t), \tag{10}$$

$$I = \sum_{i=1}^{N}\alpha_i\,\dot{q}_i - C_0\,\dot{v}\,. \tag{11}$$

In this equation, C_0 is the capacitance of the piezoelectric elements, v is the total piezoelectric voltage, and I the total outgoing current from the piezoelectric patches. In general, the piezoelectric patches are wired together in parallel. The open-circuit stiffness K_{di} of the structure is related to K_{ei}, α_i and C_0 by

$$K_{di} = K_{ei} + \frac{\alpha_i^2}{c_0}. \tag{12}$$

The eigenmode angular frequencies ω_{di} in open circuit and ω_{ei} in short circuit are defined as

$$\omega_{di} = \sqrt{\frac{K_{di}}{M_i}}, \quad \omega_{ei} = \sqrt{\frac{K_{ei}}{M_i}}. \tag{13}$$

The coupling coefficients k_i, mechanical quality factor Q_{mi} and α_i are defined as

$$k_i^2 = \frac{\alpha_i^2}{K_{di}C_0} = \frac{\omega_{di}^2 - \omega_{ei}^2}{\omega_{di}^2}, \quad Q_{mi} = \frac{K_{di}}{c_i\omega_{di}}, \quad \alpha_i = \lambda_i C_0. \tag{14}$$

The various parameters previously defined can be identified (Table 1).

Table 1
Modal parameters of the piezoelectric structure

ω_{di}	Open-circuit angular frequency for mode i	Measured
ω_{ei}	Short-circuit angular frequency for mode i	Measured
Q_{mi}	Mechanical quality factor for mode i	Measured
λ_i	Proportionality coefficient between open-circuit voltage v and beam tip deflection	Measured
C_0	Piezoelectric blocked capacitance	Measured
M_i	Modal mass for mode i	Computed from Eq. (4)
K_{di}	Open-circuit stiffness for mode i	Computed from Eq. (13)
K_{ei}	Short-circuit stiffness for mode i	Computed from Eq. (13)
c_i	Damping coefficient for mode i	Computed from Eq. (14)
α_i	Macroscopic piezoelectric coefficient for mode i	Computed from Eq. (14)

2.2. SSD switching device model

This nonlinear damping technique consists of adding a switching device in parallel with the piezoelectric elements. The current in the switching device is always zero except during the voltage inversion that takes place at each switch trigger. At each inversion, the energy extracted from the piezoelement is equal to the difference in the electrostatic energy on the piezoelectric elements before and after the voltage inversion jump. The energy dissipated in the switching device is then given by

$$\int_0^t vI\,\mathrm{d}t = \frac{1}{2}C_0\sum_k v_k^2(1-\gamma^2). \tag{15}$$

where v_k is the piezoelectric voltage just before the kth inversion and γ is the inversion coefficient. In the case of SSDI, the voltage inversion (switch) is not perfect, because one part of the energy stored on the piezoelectric element's capacitance is lost in the switching network (electronic switch, inductance). These losses are modelled by an electrical quality factor Q_i. The relationship between Q_i and the voltage of the piezoelectric element before and after the inversion process is given by

$$v_{\text{after}} = -\gamma v_{\text{before}} = -v_{\text{before}}\mathrm{e}^{-\pi/2Q_i}. \tag{16}$$

In the case of the SSDS technique, the voltage is not inverted but simply cancelled. Then the SSDS technique corresponds to the case where $\gamma = 0$. This coefficient could also be increased using external voltage sources as in the SSDV case. It can be improved as well as the corresponding damping as shown in Ref. [14]. In the following numerical simulations, the switching sequence is simply modelled at the switch triggering time by Eq. (16). It is evident that optimisation of the SSD technique (maximising the energy extracted by the switching device) is obtained by maximising the sum of the piezoelectric voltage squared before each switch.

2.3. Energy balance and energetic consideration/SSD technique

In the proposed control technique, an electric circuit is connected to the piezoelectric elements in order to perform vibration damping or harvest energy. Multiplying each term of Eq. (8) by $\dot{q}_i$, integrating over time and summing the various modes lead to energy balance of the system. This energy balance is summarised by

$$E_f = E_m + E_d + E_t \tag{17}$$

with the various energy terms detailed in Table 2. The energy supplied, E_f, by the external force is distributed as mechanical energy E_m, viscous losses E_d and transferred energy E_t. This transferred energy corresponds to the part converted into electrical energy. The goal is to maximise this energy. It is therefore necessary to establish methods to define the accurate switch trigger time that would maximise the electric power produced by the piezoelectric elements. Multiplying each of the terms of Eq. (11) by the voltage and integrating over the

Table 2
Structure energy definitions

Energy	Definition
Supplied energy	$E_f = \sum_{i=1}^{N} \varphi_i(l) \int_0^t f(t)\dot{q}_i(t)\,\mathrm{d}t$
Mechanical energy	$E_m = \frac{1}{2}\sum_{i=1}^{N} M_i\dot{q}_i^2 + \frac{1}{2}\sum_{i=1}^{N} K_{ei}q_i^2$
Viscous losses	$E_d = \sum_{i=1}^{N} \int_0^t c_i\dot{q}_i^2\,\mathrm{d}t$
Transferred energy	$E_t = \sum_{i=1}^{N} \alpha_i \int_0^t \dot{q}_i v_i\,\mathrm{d}t = \frac{1}{2}C_0 v^2 + \int_0^t vI\,\mathrm{d}t$

time shows that the transferred energy is the sum of the electrostatic energy stored on the piezoelectric elements and the energy absorbed or dissipated by the electrical device (Table 2).

3. Strategies for random vibration control

When the external force is a random function, the response of the system is a random vibration. In this case, the usual SSD strategy of control, which consists of triggering the inverting switch on each voltage extremum or strain extremum, is not necessarily optimal. More precisely in the case of a multimodal structure such as described in Section 2, many extrema appear on the voltage and deflection, which corresponds, to the various modes of the structure. The switching sequence or switching strategy that allows to maximise Σv_k^2 is not straightforward. This point has been illustrated in Fig. 2, in which it appears that the strategy of control (b) allows maximising the voltage, whereas strategy (a) allows maximising the number of inversion sequences in a given period of time.

Recent developments have been aimed at the optimal switching strategy for either vibration damping or energy harvesting. The previously investigated CPL will be briefly described and its principal drawbacks will be considered. To overcome these drawbacks, a strategy based on statistical analysis of the voltage or displacement signal will be described. The control probability and statistics strategies are based on the idea that they allow the piezoelectric voltage to reach a significant value (v_m) that is statistically probable before allowing either inverting the voltage (SSDI) or forcing it to zero (SSDS). Moreover, the switch trigger will occur on the local maximum, for which the energy stored on the piezoelement is maximum, as long as this maximum respects the previously mentioned rule.

3.1. Control Probability Law

3.1.1. Basic principle

The CPL approach previously developed [6,7] is based on a probabilistic analysis of a signal $x(t)$ that can be either the deflection $u(t)$, the square of the deflection $u^2(t)$, or the squared voltage $v^2(t)$. It is supposed that the process can be predicted and therefore could be considered as stationary on a limited period of time (a few periods of the first mode). In this case, the probability distribution function of $x(t)$ is calculated on the estimated future time window T_{es} (Fig. 4). From this function, the threshold value is defined according to a probability threshold P_{sw}. The probability P_{sw} is established arbitrarily by the user and could depend on the performance required: vibration damping or energy harvesting.

3.1.2. Estimation of the future piezoelectric voltage or deflection

When the CPL strategy is implemented on the voltage signal, the voltage threshold has to be defined according to an estimation of the open-circuited piezoelement voltage. But this voltage has to be estimated from a piecewise continuous function before the switch instant t_k such as represented on Fig. 2b or Fig. 3.

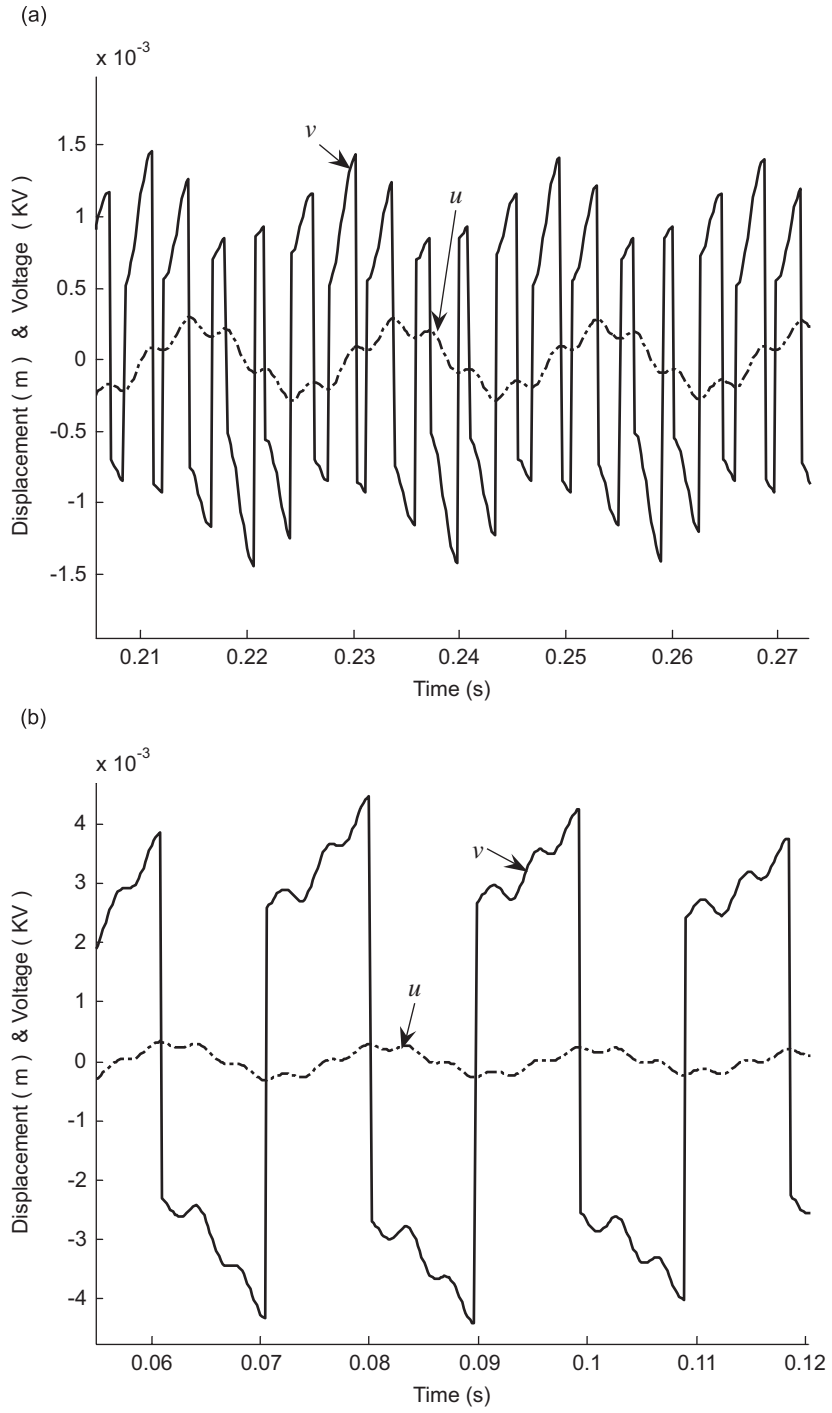

Fig. 2. Illustration of two different strategies for SSDI control: (a) original strategy with switching on each extremum; (b) alternative strategy consisting of selecting specific maximum (solid line is the piezoelement voltage; dashed line is the structure strain or deflection).

The process of voltage estimation is illustrated in Fig. 3. The estimated voltage $v_{es}(t)$ in the future time window starting at instant t_k can be theoretically obtained by Eq. (18) where t_k is the kth switching time at which the voltage switches from v_k to $-\gamma\ v_k$. In this equation, q_{ik} is the modal coordinate $q_i(t)$ of the

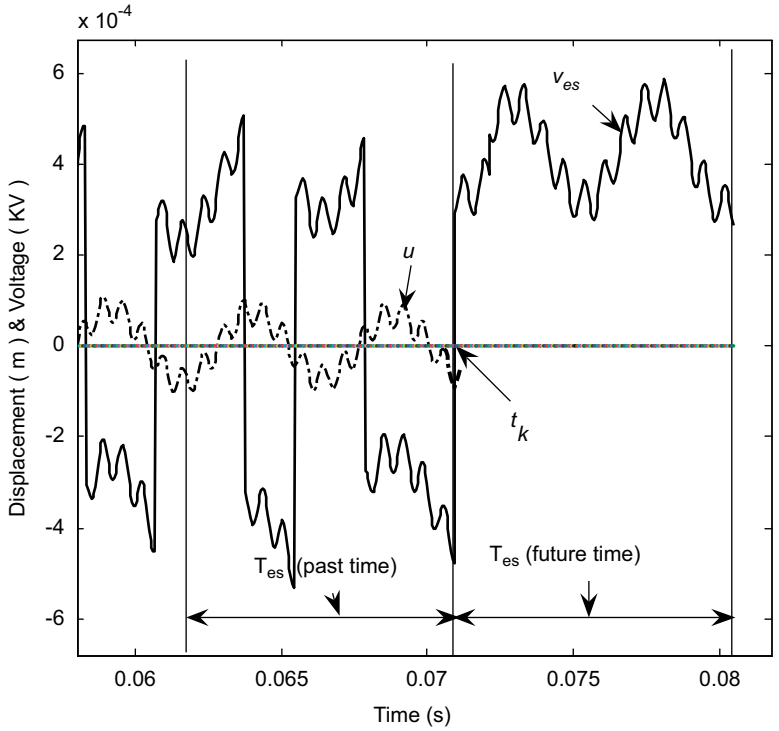

Fig. 3. Voltage estimation method after an instant of switch t_k for a time window T_{es} (the solid line is the piezoelement voltage; dash-dot line is the structure strain or deflection).

deflection at instant t_k [7].

$$v_{es}(\overset{+}{t}) = -\gamma\, v_k + \frac{1}{C_o}\sum_{i=1}^{N}\alpha_i(q_i(\bar{t}) - q_{ik}) \quad \text{with} \begin{cases} \overset{+}{t} \in [t_k,\ t_k + T_{es}]\ \text{(future)}, \\ \bar{t} \in [t_k - T_{es}, t_k]\ \text{(past)}. \end{cases} \tag{18}$$

This is reasonable when T_{es} does not exceed a few periods of the lowest resonance frequency of the structure. The value of T_{es} is set by the user. If T_{es} is too short, the control would not be sensitive to the first mode. Conversely, if T_{es} is too long, this would induce delays in the control which would therefore decrease its frequency band. Eq. (18) also means that the probability distribution function and the related probability density function of the piezoelectric voltage after the kth switching time are almost equal to before the switching time during the time window T_{es}.

In the case of deflection, this process is more trivial because the variable is a continuous function. Therefore, the signal $x(t)$ for a period T_{es} just after a switching time is supposed to be identical to the equivalent earlier window.

Experimentally, the voltage or the corresponding strain can be simply deduced from the voltage measured on an additional PZT insert left in open circuit and collocated with the principal semi-passive control PZT insert. This additional piezoelement is used as a strain sensor. If it is made with the same PZT material and with the same thickness, its output voltage v_s will be the same as the voltage that would appear on the principal PZT insert left open-circuited. This voltage is given by Eq. (19). The subsequent future estimated voltage $v_{es}(t)$ is therefore obtained by Eq. (20) from the monitoring of the sensor voltage on a time window T_{es} just before the kth switching time t_k. v_k and v_{sk} are the voltages at time t_k, respectively, on the main PZT insert and on the collocated sensor insert

$$v_s = \frac{1}{C_0}\sum_{i=1}^{N}\alpha_i q_i(t), \tag{19}$$

$$v_{es}(\overset{+}{t}) = -\gamma\, v_k + v_s(\bar{t}) - v_{sk}. \tag{20}$$

3.2. Temporal statistics method

The temporal statistics method [15] is based on statistical analysis of a signal $x(t)$. The same assumptions as in the previous case are made concerning the reproducibility of the considered process. The statistical analysis is made on an estimation of the considered $x(t)$ function on a time window T_{es} following any switching instant t_k. The estimation of the function relies on the same principle as mentioned before.

3.2.1. Statistical method on the voltage signal

This process is executed on $v^2(t)$. The time average $\mu_v{}^2$ and standard deviation $\sigma_v{}^2$ of the estimated squared voltage (Eq. (18) or Eq. (20)) are computed on a T_{es} long period window. The v_m^2 threshold will be defined by

$$v_m^2 = \mu_{v^2} + \beta\sigma_{v^2}, \tag{21}$$

where β is an arbitrary tuning coefficient. The effective variation of β depends on the statistical distribution of the estimated $v(t)$ function.

3.2.2. Statistical method on the deflection signal

The time average μ_u and standard deviation σ_u of the deflection are computed on an estimation of $u(t)$ on a T_{es} time window. In this case, the positive deflection threshold u_m will be derived as

$$u_m = |\mu_u| + \beta\sigma_u, \tag{22}$$

where β is still an arbitrary coefficient. According to the general principle aimed at triggering the switch once the voltage has reached a significant and statistically probable value, switching will occur when the absolute value of the deflection reaches the threshold u_m.

This process can also be carried out in the case of the squared deflection. As this variable remains positive, the same definitions as for Eq. (21) will be used for the threshold.

3.3. Root mean square method

This method is based on statistical analysis of signal $x(t)$ that is estimated on a time window T_{es} as in the previous cases. In this case, the root mean square or rms ψ_x of a variable $x(t)$ is computed on T_{es} window. For the various cases of $x(t)$, the x_m threshold will be defined as

$$x_m = \beta\psi_x, \tag{23}$$

where β is an arbitrary coefficient. For each signal case, Table 3 summarises the conditions in which the instants of the switch are defined.

4. Results in the case of vibration damping

4.1. Vibration damping performance analysis

In order to compare these different control approaches either for simulations or for experimental data, for vibration damping or energy harvesting, it is necessary to define quantities that will be evaluated for the sake of comparison. The quantity used is related to the deflection of structure. This quantity I_u, which is a

Table 3
Switching condition definition for each observed signal

Variable $x(t)$	Switching condition
$u(t)$	$\lvert u(t)\rvert > u_m$
$u^2(t)$	$u^2(t) > u_m^2$
$v^2(t)$	$v^2(t) > v^2{}_m$

summation in the time variable for the considered modes, is the mean-squared response of $u(x,t)$ [16] and is defined as

$$I_u = \overline{u(x,t)^2} = \lim_{\tau\to\infty}\left(\frac{1}{\tau}\int_0^\tau u^2(x,t)\,\mathrm{d}t\right) = \sum_i\sum_k\left[\varphi_i(x)\varphi_k(x)\lim_{\tau\to\infty}\left(\frac{1}{\tau}\int_0^\tau q_i(t)q_k(t)\,\mathrm{d}t\right)\right]. \tag{24}$$

This quantity will be computed in this form for simulation results. For experimental data, it will be evaluated using either the vibrometer time response or the piezoelement sensor voltage integrated on a time window whose length is large compared to the system response. The displacement damping A_u is then evaluated from these quantities, computed with the piezoelement open-circuited and then with the piezoelement driven with the desired control process, and is defined as

$$A_u = 10\,\log\left(\frac{(I_u)_{\text{controlled}}}{(I_u)_{\text{open-circuit}}}\right). \tag{25}$$

4.2. Numerical simulations results

In this paragraph, a random force is applied to the free end of the clamped beam. This force is applied on a time domain lasting 200 periods of the lowest resonance frequency of the system. The model (Eqs. (8) and (11) principally) is simulated by numerical integration using the fourth-order Runge–Kutta algorithm. The simulations are carried out using the various methods described in Section 3. The observation time window T_{es} has to be twice the period of the lowest resonance frequency to give satisfactory results. This time should be sufficiently long to obtain a realistic image of the deflection especially for the lowest frequency mode and sufficiently short to maintain a good frequency response of the control. The considered structure and the corresponding numerical data calculated using the expressions detailed in Section 2 are gathered in Tables 4 and 5, respectively.

Fig. 5 shows the variations of the displacement damping A_u versus both the probability P_{sw} (for CPL method) and the β coefficient (for either rms or statistics method). For the various methods, the signal considered for the definition of the threshold is $v(t)^2$. Depending on β and P_{sw}, the statistics, rms or CPL methods lead to better results than simple SSDI and the damping and consequently the energy extraction are better. Note that simple SSDI consists of switching blindly on each extremum of the considered reference signal (either u or v^2 or u^2). The optimum displacement damping is –8.0 dB whereas it is –6.4 dB in simple SSDI. The applicable interval of β, for which the displacement damping A_u stays minimum, is very large for the statistics method. Conversely, the other methods are more sensitive to the adjustment of either β or P_{sw}. This is a good advantage for the statistics method because, for a high range of excitation signals, it is not necessary to regulate β for each force to have optimum damping. This indicates that the target of the extremum in the case of statistics is better. The curve representative of the statistics method shows a sharp

Table 4
Characteristics of the experimental structure

Plate material	Steel
Plate dimensions (mm^3)	$180 \times 90 \times 2$
Piezoelectric material	P189 (Saint-Gobain—quartz)
Number of piezoelements	2
Piezoelements position	12 mm from the clamping end
Piezoelements dimensions (mm^3)	$40 \times 90 \times 0.3$
Piezoelements capacitance: C_0 (nF)	74
Inversion coefficient: γ	0.6
Open-circuit resonance frequencies (Hz)	56.48; 321; 890
Coupling coefficients: k_i	0.0959; 0.0663; 0.0265

Table 5
Modal parameters of the considered system

	First mode	Second mode	Third mode
M_i (g)	71.6	72.2	71.5
K_{di} (N/m)	7800	319 000	2 398 800
K_{ei} (N/m)	7700	317 600	2 397 100
α_i (N/V)	0.0023	0.0102	0.0111

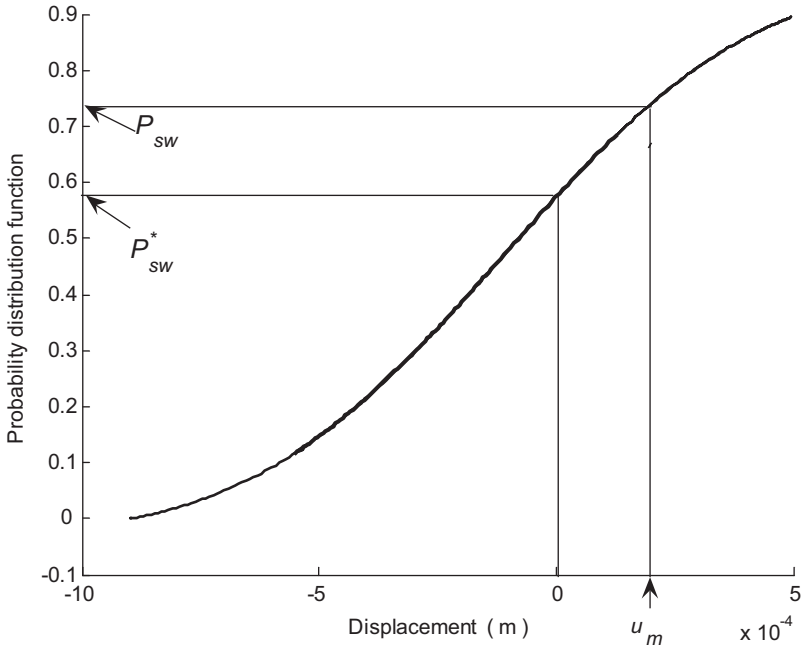

Fig. 4. Determination of the u_m threshold for the CPL method. Vertical and horizontal axes are the probability and the free-end deflection of the beam, respectively. In this figure $P_{sw}{}^*$ corresponds to $u_m = 0$.

decrease in the displacement damping for β values larger than 2. This is very understandable, because in this simulation the quality factors of the various modes are close to $Q_m = 500$ and consequently the signal is very well filtered and locally close to a sinusoid.

Fig. 6 shows the same kind of comparison but in this case the considered signal is the deflection signal $u(x, t)$. For the statistics and rms methods, a large domain of β permits good damping. Conversely, for the CPL method, two probability thresholds have to be properly tuned on each side apart from $P_{sw} = 0.5$ which corresponds to the median ($u(x, t) = 0$). This is a drawback for the probability method when we use the deflection signal to make the switch. For the middle value (P_{sw} around 0.5), u_m is very much smaller (Fig. 4) and switching is not optimum. If P_{sw} is close to 0 or 1, this corresponds to the extremum of the deflection, which does not occur often enough to ensure good energy extraction and therefore good global deflection damping. The other methods are affected similarly when β is higher than $\sqrt{2}$ which would correspond to the extrema for a pure sinusoidal signal.

Fig. 7 illustrates this latter point. It shows the variations of the displacement damping (A_u) versus the number of switches, in the total time window. This number is naturally dependent on the control method and for the statistics method depends on the β coefficient. The minimum value of A_u is –7.0 dB for 290 switching sequences for the statistics method. In the case of simple SSDI (switch on each extremum), the number of

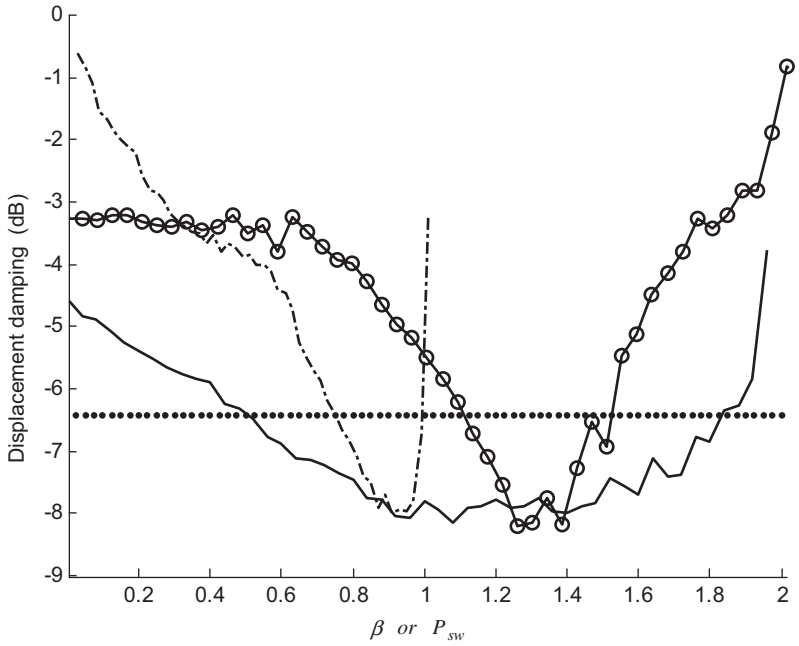

Fig. 5. Variations of the displacement damping (A_u) in dB versus the probability threshold (P_{sw}) or the β coefficients for the various methods. The observed signal is the squared piezoelectric voltage (——— statistics, – · – · – probability, —⊖— rms, ▪ ▪ ▪ ▪ simple SSDI).

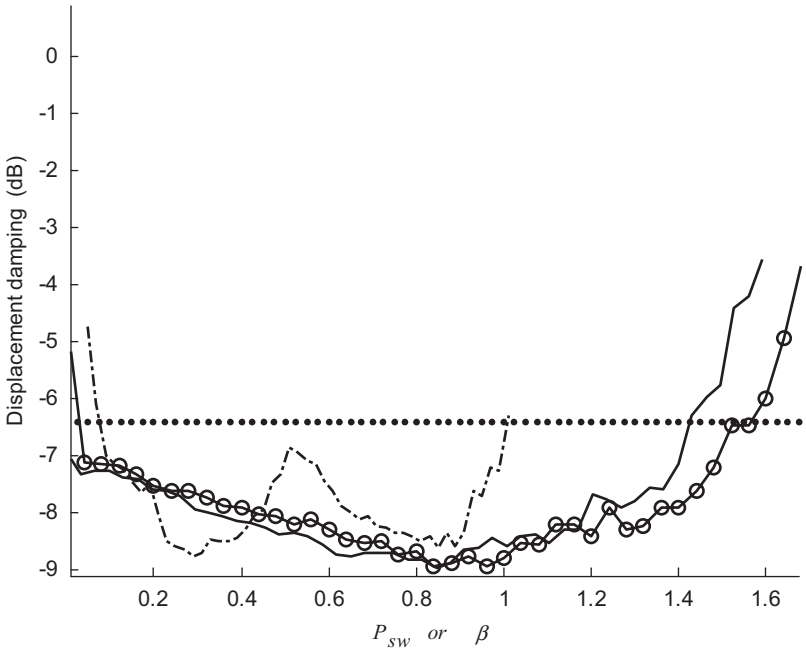

Fig. 6. Variations of the displacement damping (A_u) in dB versus the probability threshold (P_{sw}) or the β coefficients for the various methods. The observed signal is the beam tip deflection $u(L, t)$ (——— statistics, – · – · – probability, —⊖— rms, ▪ ▪ ▪ ▪ simple SSDI).

switches is 2990 for a –4.6 dB displacement damping for the same total time window. This figure illustrates that it is not the amount of switching sequences, which is important, but much more the instant of the switch. It illustrates and quantifies the trade-off that was set by Fig. 2.

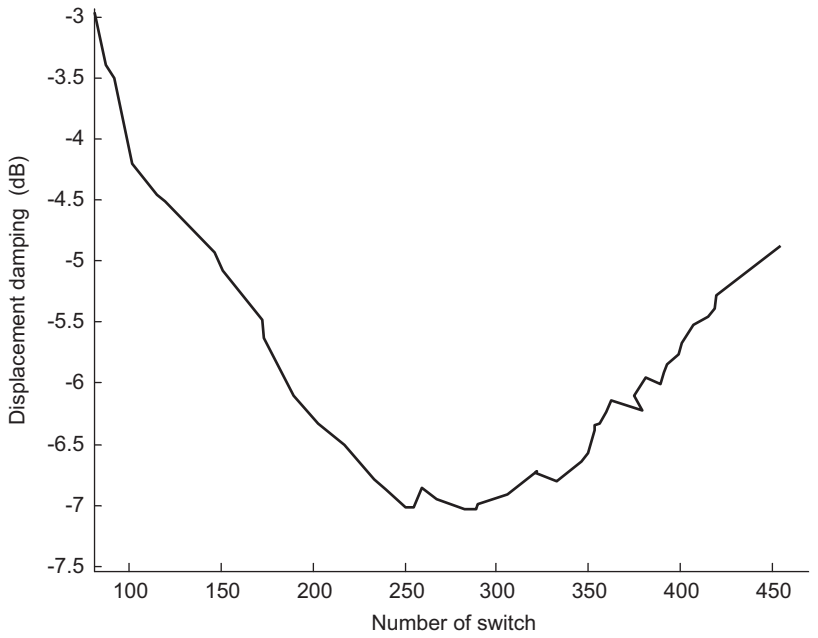

Fig. 7. Illustration of the displacement damping variations (A_u) versus the number of switching sequences for the statistics method for a given total time window and for different values of β.

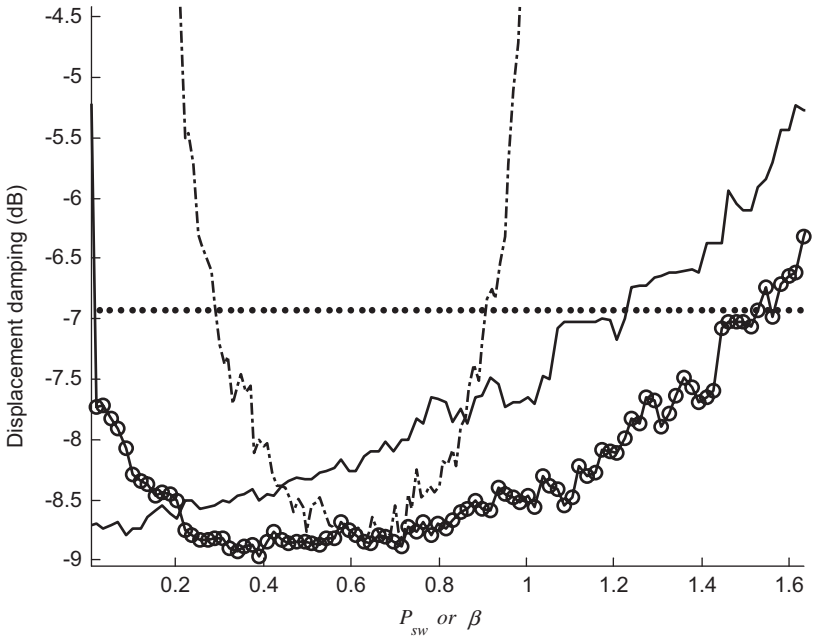

Fig. 8. Variations of the displacement damping (A_u) in dB versus the probability threshold (P_{sw}) or the β coefficients for the various methods. The observed signal is the squared beam tip deflection $u(L,t)^2$ (—— statistics, – · – probability, —o— rms, ▪ ▪ ▪ simple SSDI).

Fig. 8 is similar to Fig. 5 except that the signal considered is the square of the deflection. Another slight difference is a lower mechanical quality factor ($Q_m = 250$). In this case, the rms method tends to a lower sensitivity of the β coefficient and the P_{sw} coefficient tuning of the CPL method tends to be less sensitive.

Fig. 9 shows the influence of the considered signal (either u or u^2or v^2) for the statistical method. In these cases, the natural mechanical quality factor is 500. The displacement damping is plotted as a function of β. For the various signals, the optimal damping is almost the same. The main difference is related to the acceptable bandwidth for the β adjustment parameters. It appears that using $u^2(t)$ leads to damping very little dependent on β.

4.3. Experimental set-up and results

The experimental set-up considered is a steel beam equipped with piezoelectric inserts. This structure corresponds to the description given in Table 4. Table 5 data are representative of the real structure as described in Ref. [7]. The proposed control strategies are implemented using a laboratory PC-based real-time DSP controller environment (dSPACE DSP board DS-1104). Either the voltage or the displacement signals are sampled by the board as input data. Local extrema are numerically localised and the corresponding levels compared to the thresholds calculated as defined previously. According to the proposed method, the switch trigger is generated by the digital output of the control board, connected on a SSDI switching device built as described in Ref. [8]. The displacement sensor used is a simple piezoelectric insert collocated with the main insert. The sensor thickness and material are similar to the control insert and therefore it generates the same open-circuit voltage (amplitude and phase).

Control strategy programming and implementation are done using the Matlab/Simulink^{TM} software environment and using the dSPACE Real-Time Workshop for real-time computing and input/output control. Note that only $u(t)$ has been implemented as the observation signal for practical purposes. Since it is not necessary to estimate the signal in the future and by using a displacement sensor, it is realised very easily. It is studied during the T_{es} time window (sliding window) just before the present time and the threshold level u_m is calculated as defined previously for each method, then it is compared to the observed signal to define the instant of the next switch.

Excitation of the beam is carried out using an electromagnet driven by an audio amplifier, by a random noise during a 50 s sequence generated by the dSPACE board. Actually, the noise sequence was generated once

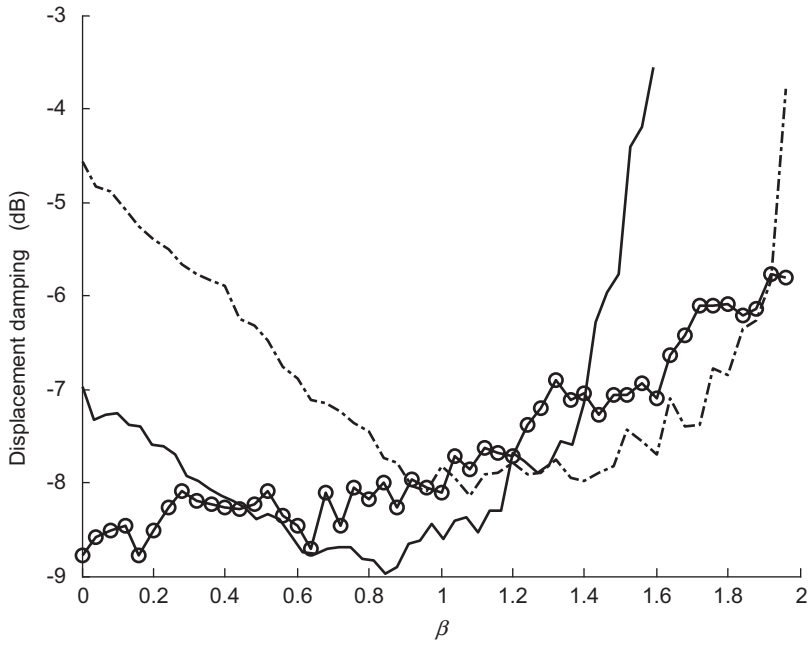

Fig. 9. Displacement damping (A_u) in dB versus the β coefficient with the statistics method for the three observed signals (u, u^2, v^2). (—— deflection signal, – · – square of voltage, —⊟— square of deflection).

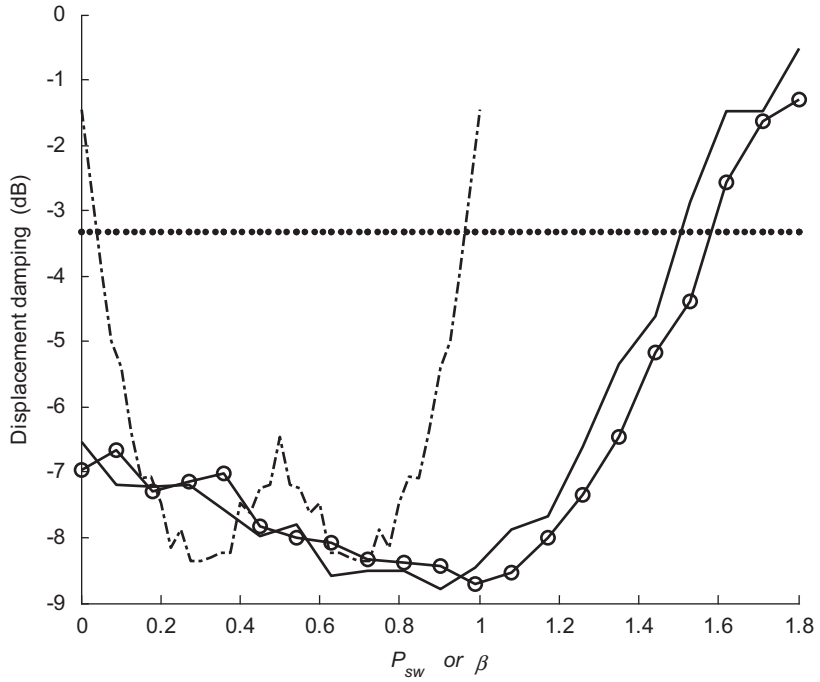

Fig. 10. Experimental results for the displacement damping (A_u) in dB versus probability (P_{sw}) and β coefficients (——— statistics, – · – probability, —○— rms, ▪ ▪ ▪ simple SSDI).

and was replayed for all of the tests for comparison. The estimation time window used is exactly twice the lowest mode period.

The displacement damping A_u is computed using the image of $u(t)$ given by the collocated piezoelectric deflection sensor insert. Fig. 10 shows the experimental results for the statistics, CPL, and rms methods and simple SSDI (switch on each extremum). These results have to be compared with Fig. 6. Experimental and simulated data agree quite well. The weak sensitivity of the control to the β coefficient is confirmed according to the large range of β (approx $0.2<\beta<1.2$) which allows nearly optimal displacement damping for statistics or for rms methods. Fig. 11 illustrates the beam tip velocity with and without the statistics ($\beta = 0.8$) SSDI control. The damping achieved for a large band semi-passive method (no operating energy) is remarkable. In the simulation and experiment, there is not much difference in performance between the statistics and rms methods, because the mean value of the deflection signals is very small.

5. Conclusions

The SSDI semi-passive nonlinear control technique is interesting for structural damping applications because it presents simultaneously good damping performance, good robustness and very low power requirements. The main limitations are related to the case of complex or random excitation where the synchronisation on the strain extremum is not trivial.

It was shown that either a probability or statistical analysis of the strain could allow the definition of criteria to identify more accurately the relevant switching instants. However, these methods require a little knowledge of the signal, which results in the definition of a tuning parameter: P_{sw} for the CPL method or β for the statistics or rms methods. The proposed work shows that for the latter methods, this adjustment can be made very coarse. Moreover, calculation of the average value or the rms value of a given signal can be easily implemented either using a numerical method as in the proposed experimental work or using analogue low-power electronic circuits. It was also shown that for damping purposes the best results could be obtained using either an image of the strain (displacement) or the square of this value. This is easier to implement than the

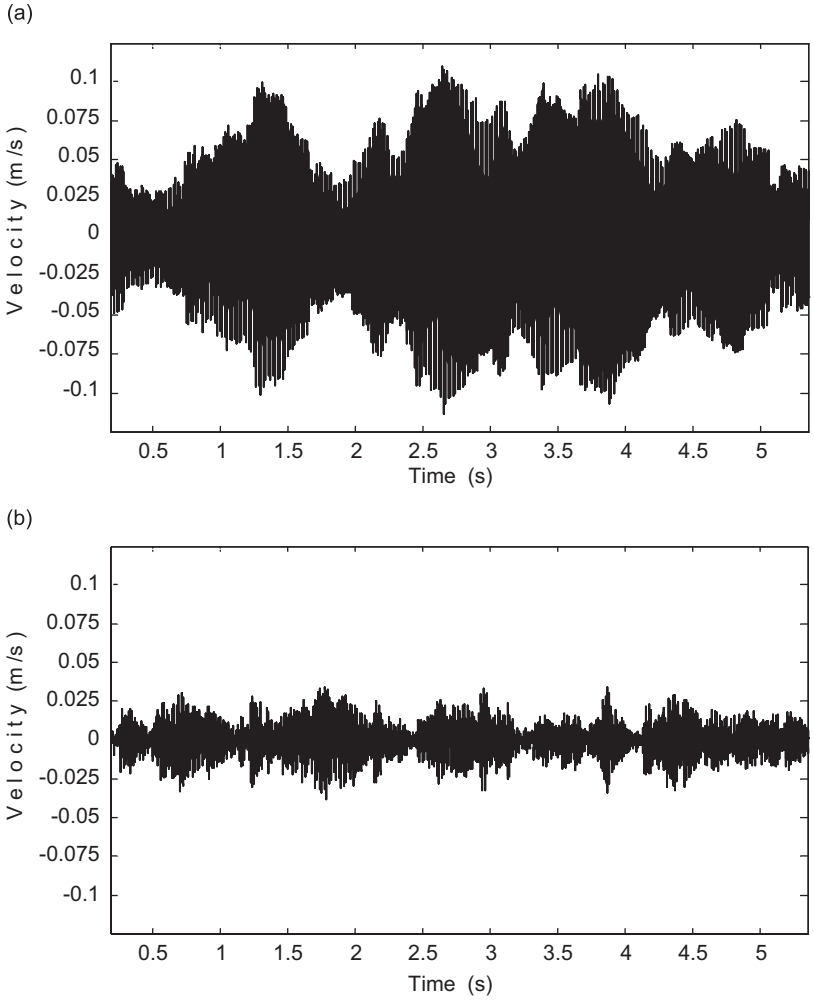

Fig. 11. Free end velocity of the beam: (a) without control and (b) in the case of SSDI control with the statistics method.

reconstructed voltage signal. The main drawback in this case is the use of a specific sensor collocated with the piezoelectric insert. Global displacement damping close to 10 dB can be obtained using these approaches, nearly twice the damping that can be achieved using classic SSDI techniques. Finally, it is important to consider that these techniques are simple enough to be self-powered. In the future, adaptation of coefficient β to each excitation force should be studied in order to attain optimum switch damping.

References

[1] D. Guyomar, A. Badel, E. Lefeuvre, C. Richard, Toward energy harvesting using active materials and conversion improvement by nonlinear processing, *IEEE Transactions on Ultrasonics Ferroelectrics and Frequency Control* 52 (4) (2005) 584–595.

[2] A. Badel, D. Guyomar, E. Lefeuvre, C. Richard, Efficiency enhancement of a piezoelectric energy-harvesting device in pulsed operation by synchronous charge inversion, *Journal of Intelligent Material Systems and Structures* 16 (10) (2005) 889–901.

[3] E. Lefeuvre, A. Badel, C. Richard, D. Guyomar, Piezoelectric energy harvesting device optimization by synchronous electric charge extraction, *Journal of Intelligent Material Systems and Structures* 16 (10) (2005) 865–876.

[4] C.L. Davis, G.A. Lesieutre, An actively tuned solid-state vibration absorber using capacitive shunting of piezoelectric stiffness, *Journal of Sound and Vibration* 232 (2000) 601–617.

[5] W.W. Clark, Vibration control with state-switching piezoelectric material, *Journal of Intelligent Material Systems and Structures* 11 (2000) 263.

[6] A. Badel, Récupération D'énergie et Contrôle Vibratoire par Eléments Piézoélectriques Suivant une Approche Non-linéaire, PhD Thesis, Université de Savoie, 2005, p. 161.
[7] D. Guyomar, A. Badel, Nonlinear semi-passive multimodal vibration damping: an efficient probabilistic approach, *Journal of Sound and Vibration* 294 (2006) 249–268.
[8] C. Richard, D. Guyomar, D. Audigier, H. Bassaler, Enhanced semi-passive damping using continuous switching of a piezoelectric device on an inductor, *Proceedings SPIE Smart Structures and Materials Conference—Passive Damping and Isolation*, Vol. 3989, Newport, 2000, p. 288.
[9] A. Badel, A. Benayad, E. Lefeuvre, L. Lebrun, C. Richard, D. Guyomar, Single crystals and nonlinear process for outstanding vibration-powered electrical generators, *IEEE Transactions on Ultrasonics Ferroelectrics and Frequency Control* 53 (4) (2006) 673–684.
[10] E. Boucher, D. Guyomar, L. Lebrun, B. Guiffard, G. Grange, Effect of (Mn, F) and (Mg, F) co-doping on dielectric and piezoelectric properties of lead zirconate titanate ceramics, *Journal of Applied Physics* 92 (9) (2002) 5437–5442.
[11] C. Richard, D. Guyomar, D. Audigier, G. Ching, Semi passive damping using continuous switching of a piezoelectric device, *Proceedings SPIE Smart Structures and Materials Conference—Passive Damping and Isolation*, San Diego, Vol. 3672, 1999, p. 104.
[12] L.R. Corr, W.W. Clark, A novel semi-active multi-modal vibration control law for a piezoceramic actuator, *Transactions of the ASME* 125 (2003) 214–222.
[13] K.G. McConnell, *Vibration Testing Theory and Practice*, Wiley, New York, 1995.
[14] A. Badel, G. Sebald, D. Guyomar, M. Lallart, E. Lefeuvre, C. Richard, J. Qiu, Piezoelectric vibration control by synchronized switching on adaptive voltage sources: towards wideband semi-active damping, *Journal of Acoustical Society of America* 119 (5) (2006) 2815–2825.
[15] L. Meirovitch, *Analytical Methods in Vibrations*, Macmillan Company, New York, 1967.
[16] W.T. Thomson, *Theory of Vibration with Applications*, Prentice-Hall, Englewood Cliffs, NJ, 1981.